mathematics

MDPI

Article

Analytical Investigation of Some Time-Fractional Black–Scholes Models by the Aboodh Residual Power Series Method

Muhammad Imran Liaqat [1,2], Ali Akgül [3,4,5,*] and Hanaa Abu-Zinadah [6]

[1] Abdus Salam School of Mathematical Sciences, Government College University, 68-B, New MuslimTown, Lahore 54600, Pakistan
[2] National College of Business Administration & Economics, Lahore 54000, Pakistan
[3] Department of Computer Science and Mathematics, Lebanese American University, Beirut P.O. Box 13-5053, Lebanon
[4] Department of Mathematics, Art and Science Faculty, Siirt University, Siirt 56100, Turkey
[5] Mathematics Research Center, Department of Mathematics, Near East University, Near East Boulevard, Nicosia, Mersin 99138, Turkey
[6] Department of Statistics, College of Science, University of Jeddah, Jeddah 21959, Saudi Arabia
* Correspondence: aliakgul@siirt.edu.tr

Abstract: In this study, we use a new approach, known as the Aboodh residual power series method (ARPSM), in order to obtain the analytical results of the Black–Scholes differential equations (BSDEs), which are prime for judgment of European call and put options on a non-dividend-paying stock, especially when they consist of time-fractional derivatives. The fractional derivative is considered in the Caputo sense. This approach is a combination of the Aboodh transform and the residual power series method (RPSM). The suggested approach is based on a new version of Taylor's series that generates a convergent series as a solution. The advantage of our strategy is that we can use the Aboodh transform operator to transform the fractional differential equation into an algebraic equation, which decreases the amount of computation required to obtain the solution in a subsequent algebraic step. The primary aspect of the proposed approach is how easily it computes the coefficients of terms in a series solution using the simple limit at infinity concept. In the RPSM, unknown coefficients in series solutions must be determined using the fractional derivative, and other well-known approximate analytical approaches like variational iteration, Adomian decomposition, and homotopy perturbation require the integration operators, which is challenging in the fractional case. Moreover, this approach solves problems without the need for He's polynomials and Adomian polynomials, so the small size of computation is the strength of this approach, which is an advantage over various series solution methods. The efficiency of the suggested approach is verified by results in graphs and numerical data. The recurrence errors at various levels of the fractional derivative are utilized to demonstrate the convergence evidence for the approximative solution to the exact solution. The comparison study is established in terms of the absolute errors of the approximate and exact solutions. We come to the conclusion that our approach is simple to apply and accurate based on the findings.

Keywords: Aboodh transform; Black–Scholes differential equations; Caputo derivative; residual power series method

MSC: 26A33; 40C15

check for updates

Citation: Liaqat, M.I.; Akgül, A.; Abu-Zinadah, H. Analytical Investigation of Some Time-Fractional Black–Scholes Models by the Aboodh Residual Power Series Method. *Mathematics* **2023**, *11*, 276. https://doi.org/10.3390/math11020276

Academic Editor: Lihua Wang

Received: 21 December 2022
Revised: 29 December 2022
Accepted: 30 December 2022
Published: 5 January 2023

Copyright: © 2023 by the authors. Licensee MDPI, Basel, Switzerland. This article is an open access article distributed under the terms and conditions of the Creative Commons Attribution (CC BY) license (https://creativecommons.org/licenses/by/4.0/).

1. Introduction

Many scientists and researchers have been drawn to fractional calculus (FC) in recent decades because it is commonly used in scientific contexts such as engineering, image processing, physics, biochemistry, biology, fluid mechanics, and entropy theory [1–5]. For the most recent research advances in the field of FC, see [6–8]. There are numerous techniques to

define fractional derivatives, but not all of them are typically applied. The most-prominent categories are Atangana–Baleanu, Riemann–Liouville (R-L), Caputo–Fabrizio, conformable operators, and the Caputo derivative (CD) [9–13]. Fractional derivatives may simulate and study complex systems with complex non-linear processes and higher-order behaviors, making them sometimes preferable to integer-order derivatives for modeling. There are primarily two reasons for this. First, rather than being limited to an integer order, we can choose any order for the derivative operator. Second, non-integer-order derivatives are affected by both past and present conditions when the system has long-term memory.

The primary components of FC, which is the generalized version of classical calculus and has piqued the interest of numerous academics and scientists due to its wide range of applications, are fractional-order differential equations (FODEs). FODEs are frequently used for their logical support in the mathematical framework of physical problems, including technology, health care, monetary markets, and decision theory [14–18]. As a result, the solutions of FODEs are significant and useful. Applications regularly face FODEs that are too complex for exact solutions. Under the specified initial or boundary conditions, approximate numerical methods present a potent alternative tool for solving FODEs. Several approximate numerical methods, including the pseudo-spectral [19], the fractional reproducing kernel [20], the differential transform [21], the operational matrix [22], the variational iteration [23], the Haar wavelet collocation [24], the finite difference [25], the fractional power series [26], the Chebyshev polynomials [27], the residual power series [28], differential quadrature [29], Bezier [30], and the natural transform homotopy perturbation [31], have been described in recent years for solving FODEs.

The pricing of financial derivatives is a topic that has generated a great deal of interest and literature. A financial derivative is an asset whose price is based on the value of another asset. Frequently, a stock or bond serves as the underlying asset. Financial derivatives are not a completely novel concept. It is generally agreed that Charles Castelli's work, which was published in 1877, was the first attempt at contemporary derivative pricing, despite some historical controversy regarding the exact year of the birth of financial derivatives [32]. Castelli's book described the general introduction and ideas of hedging and speculative trading, but it lacked a mathematical model.

The first widely used mathematical method to calculate the theoretical value of an option contract using prevailing equity markets' predicted dividends, the option's strike price, projected interest rates, time till cessation, and expected unpredictability was the Black–Scholes (BS) model, developed in 1997 by Fischer Black, Robert Merton, and Myron Scholes. The Pricing of Options and Corporate Liabilities by Black and Scholes, published in the *Journal of Political Economy* in 1973, provided the initial formulation of the equation. Robert C. Merton contributed to the editing of that document. Later that year, he wrote his own work, "Theory of Rational Option Pricing", expanding the model's mathematical capabilities and applications while also coining the term "BS theory of options pricing" [33].

One of the most-significant mathematical representations of a financial market is the BS equation. The value of financial derivatives is controlled by a second-order parabolic partial differential equation. Many different commodities and payout structures have been used in the BS model for pricing stock options. The following equation describes the BS model for the value of an option [34]:

$$\frac{\partial^{\hbar}\Omega(\alpha,\tau)}{\partial\tau^{\hbar}}+\frac{\omega^2\alpha^2}{2}\frac{\partial^2\Omega(\alpha,\tau)}{\partial\alpha^2}+\Theta(\tau)\alpha\frac{\partial\Omega(\alpha,\tau)}{\partial\alpha}-\Theta(\tau)\Omega(\alpha,\tau)=0,\ (\alpha,\tau)\in\mathcal{R}^{+}\times(0,Y), \tag{1}$$

$\Omega(\alpha,\tau)$ is the European offer's value at the fundamental market cap of α and time τ; the fluctuation component of the company's shares, often referred to as ω, quantifies the variance of the stock's return; Y is the expiration date; $\Theta(\tau)$ is the risk-free interest rate. $\Omega_c(\alpha,\tau)$ and $\Omega_p(\alpha,\tau)$, correspondingly, stand for the call and put values on European options. Then, the payoff functions are given by $\Omega_c(\alpha,\tau)=\max(\alpha-W,0)$, $\Omega_p(\alpha,\tau)=\max(W-\alpha,0)$, where W indicates the termination price for the option and the function $\max(\alpha,0)$ gives the larger value between α and 0. The important financial view of the BS

equation is that it minimizes risk by allowing for the prudent selection of purchasing and selling the stock under scrutiny. It is a sign that, according to the BS financial model, there is only one correct price for the option. The important financial view of the BS equation is that it minimizes risk by allowing for the prudent selection of purchasing and selling the stock under scrutiny. It is a sign that, according to the BS financial model, there is only one correct price for the option. In this article, a fractional model that may be used to model the pricing of various financial derivatives is presented.

The time-fractional BSDEs have been studied using a number of approaches [35–45]. These approaches require much computation. In this study, we used ARPSM [46], a new, straightforward approach for solving BSDEs. This approach combines the Aboodh transform (AT) and the RPSM. The set of rules for this approach are as follows: First, apply the AT to BSDEs, and then, introduce the solution of BSDEs into the novel space using the novel form of Taylor's series. This series' coefficients are established using a novel concept. In the end, the problem was solved in the actual space by using the inverse AT. The proposed approach has an edge over the homotopy perturbation method (HPM) and the Adomian decomposition method (ADM) due to its prowess in solving problems without the use of He's and Adomian polynomials. This approach has the advantage of not requiring any physical parameter assumptions to solve the problem. The key benefit of the suggested approach is how easily the coefficients in terms of a series solution can be calculated using merely the concept of a limit at infinity. Other well-known analytical approximation methods, such as the variational iteration method (VIM), ADM, and HPM, necessitate the use of integration operators, whereas the RPSM must find the fractional derivative each time to find the unknown coefficients in series solutions, which is difficult in the fractional case. Therefore, the ARPSM has various advantages over other series solution methods. The recurrence error (Rec. E) and absolute error (Abs. E) are used to graphically and numerically compare the exact and approximative solutions. The Rec. E and Abs. E verified the convergence rates and accuracy of the approximation solutions in order to show the effectiveness of the proposed approach.

The paper's structure is as follows: In the section that follows, we use a number of important definitions and conclusions from the theory of FC. The main concept of the ARPSM is examined in Section 3 in order to establish the analytical solutions of the time-fractional BSDEs. Section 4 investigates the potential, capability, and simplicity of the suggested approach using three numerical models. In Section 5, graphics and tables are used to investigate the results obtained by the ARPSM. Section 6, towards the end, gives the conclusion.

2. Preliminaries

This section contains a number of definitions, features, and some helpful findings that form the foundation of the new approach. The AT is derived using the conventional Fourier integral. In order to simplify the method for solving ordinary and partial differential equations in the specified time periods, Khalid Aboodh founded the AT in 2013 [47]. The Elzaki and Laplace transforms have the closest relationships with this integral transform. The key notations, the fundamental definition of the AT, and a few features are covered below:

Definition 1. *[47] Assume that the AT existence axioms are satisfied by* $\Omega(\alpha,\tau)$*. The AT of* $\Omega(\alpha,\tau)$ *for* $\tau \geq 0$ *is then defined as follows:*

$$\mathcal{A}[\Omega(\alpha,\tau)] = \aleph(\alpha,\theta) = \frac{1}{\theta}\int_0^\infty \Omega(\alpha,\tau)e^{-\theta\tau}d\tau,\ \xi_1 \leq \theta \leq \xi_2, \tag{2}$$

and the inverse of the AT is defined by:

$$\mathcal{A}^{-1}[\aleph(\alpha,\theta)] = \Omega(\alpha,\tau) = \frac{1}{2\pi\iota}\int_{q-\iota\infty}^{q+\iota\infty} \theta e^{\theta\tau}\aleph(\alpha,\theta)d\theta. \tag{3}$$

Lemma 1. *[46–49] Assume that the AT existence axioms are satisfied by $\Omega_1(\alpha,\tau)$ and $\Omega_2(\alpha,\tau)$. Assume that $\mathcal{A}[\Omega_1(\alpha,\tau)] = \aleph_1(\alpha,\theta)$, $\mathcal{A}[\Omega_2(\alpha,\tau)] = \aleph_2(\alpha,\theta)$, and λ_1, λ_2 are constants. Then, the following characteristics are satisfied:*

(i) $\mathcal{A}[\lambda_1\Omega_1(\alpha,\tau) + \lambda_2\Omega_2(\alpha,\tau)] = \lambda_1\aleph_1(\alpha,\theta) + \lambda_2\aleph_2(\alpha,\theta)$;

(ii) $\mathcal{A}^{-1}[\lambda_1\aleph_1(\alpha,\theta) + \lambda_2\aleph_2(\alpha,\theta)] = \lambda_1\Omega_1(\alpha,\tau) + \lambda_2\Omega_2(\alpha,\tau)$;

(iii) $\vartheta_0(\alpha) = \lim_{\theta\to\infty}\theta^2\aleph(\alpha,\theta) = \Omega(\alpha,0)$;

(iv) $\mathcal{A}[D_\tau^{\hbar}\Omega(\alpha,\tau)] = \theta^{\hbar}\aleph(\alpha,\theta) - \sum_{\kappa=0}^{\nu-1}\frac{\Omega^{(\kappa)}(\alpha,0)}{\theta^{\kappa-\hbar+2}},\ \nu-1<\hbar\le\nu,\ \nu\in\mathbb{N}$;

(v) $\mathcal{A}[D_\tau^{\nu\hbar}\Omega(\alpha,\tau)] = \theta^{\nu\hbar}\aleph(\alpha,\theta) - \sum_{\kappa=0}^{\nu-1}\theta^{\hbar(\nu-\kappa)-2}D_\tau^{\kappa\hbar}\Omega(\alpha,0),\ 0<\hbar\le 1$.

Definition 2. *[46] The CD of $\Omega(\alpha,\tau)$ of order $\hbar$ is defined as follows:*

$$D_\tau^{\hbar}\Omega(\alpha,\tau) = \mathcal{J}_{\hbar}^{\kappa-\hbar}\Omega^{(\kappa)}(\alpha,\tau),\ \tau\ge 0,\ \kappa-1<\hbar\le\kappa, \tag{4}$$

where $\mathcal{J}_\tau^{\kappa-\hbar}$ is the R-L integral of $\Omega(\alpha,\tau)$.

Theorem 1. *[46] Assume that the multiple fractional power series (MFPS) representation for the function $\mathcal{A}[\Omega(\alpha,\tau)] = \aleph(\alpha,\theta)$ is given by*

$$\aleph(\alpha,\theta) = \sum_{\nu=0}^{\infty}\frac{\vartheta_\nu(\alpha)}{\theta^{\nu\hbar+2}},\ \theta>0, \tag{5}$$

then we have

$$\vartheta_\nu(\alpha) = D_\tau^{\nu\hbar}\Omega(\alpha,0), \tag{6}$$

where $D_\tau^{\nu\hbar} = D_\tau^{\hbar}.D_\tau^{\hbar}\dots D_\tau^{\hbar}(\nu-times)$.

The conditions for the convergence of $\aleph(\alpha,\theta) = \sum_{\nu=0}^{\infty}\frac{\vartheta_\nu(\alpha)}{\theta^{\nu\hbar+2}}$ is determined in the following theorem.

Theorem 2. *[46] Let $\mathcal{A}[\Omega(\alpha,\tau)] = \aleph(\alpha,\theta)$ be denoted as the new form of the MFPS explained in Theorem 1. If $|\theta^2\mathcal{A}[D_\tau^{(\kappa+1)\hbar}\Omega(\alpha,\tau)]| \le \mathcal{W}$, on $0<\theta\le b$ with $0<\hbar\le 1$, then the remainder $R_\kappa(\alpha,\theta)$ of the new form of the MFPS satisfies the following inequality:*

$$|R_\kappa(\alpha,\theta)| \le \frac{\mathcal{W}}{\theta^{(\kappa+1)\hbar+2}},\ 0<\theta\le b. \tag{7}$$

3. The Algorithms for the Solution of BSDEs by ATRPM

This section examines the algorithms for using the proposed approach to find a solution to the BS model. Applying the AT to the BS model and then considering the MFPS as the BS model's new space solution constitutes the main idea of the ARPSM. The way in which the coefficients of this series utilize the limit idea is the main difference between the ARPSM and the RPSM. The generated consequents are then transformed into real space using the inverse AT. The algorithms for using the ARPSM to find solutions are as follows:

Step 1. Equation (1) can be written as follows:

$$D_\tau^{\hbar}\Omega(\alpha,\tau) - f\left(\Omega(\alpha,\tau), \frac{\omega^2\alpha^2\partial^2\Omega(\alpha,\tau)}{2\partial\alpha^2}, \Theta(\tau)\alpha\frac{\partial\Omega(\alpha,\tau)}{\partial\alpha}, \Theta(\tau)\Omega(\alpha,\tau)\right) = 0. \tag{8}$$

Step 2. By considering $\mathcal{A}$ on both sides of Equation (8), we obtain the following:

$$\aleph(\alpha,\theta) - \frac{\Omega(\alpha,0)}{\theta^2} - \frac{1}{\theta^{\hbar}}\mathcal{M}(\alpha,\theta) = 0, \tag{9}$$

where

$$\aleph(\alpha,\theta) = \mathcal{A}[\Omega(\alpha,\tau)],$$

and

$$\mathcal{M}(\alpha,\theta) = \mathcal{A}\Big[f\Big(\Omega(\alpha,\tau), \frac{\omega^2\alpha^2\partial^2\Omega(\alpha,\tau)}{2\partial\alpha^2}, \Theta(\tau)\alpha\frac{\partial\Omega(\alpha,\tau)}{\partial\alpha}, \Theta(\tau)\Omega(\alpha,\tau)\Big)\Big].$$

Step 3. Assume that the solution of Equation (9) is the series below:

$$\aleph(\alpha,\tau) = \sum_{\nu=0}^{\infty} \frac{\vartheta_\nu(\alpha)}{\theta^{\nu\alpha+2}},\ \theta > 0, \tag{10}$$

Step 4. We obtained the following as a result of using Lemma 1(iii).

$$\vartheta_0(\alpha) = \lim_{\theta\to\infty} \theta^2\aleph(\alpha,\theta) = \Omega(\alpha,0) = 0. \tag{11}$$

Step 5. Define the κth truncated expansion of $\aleph(\alpha,\theta)$ as

$$\aleph_\kappa(\alpha,\theta) = \frac{\vartheta_0(\alpha)}{\theta^2} + \sum_{\nu=1}^{\kappa} \frac{\vartheta_\nu(\alpha)}{\theta^{\nu\hbar+2}}. \tag{12}$$

Step 6. Introduce the Aboodh residual function $(\mathcal{ARF})$ of Equation (9) and κth $\mathcal{ARF}$, respectively, as follows:

$$\mathcal{A}[Res(\alpha,\theta)] = \aleph(\alpha,\theta) - \frac{\vartheta_0(\alpha)}{\theta^2} - \frac{1}{\theta^{\hbar}}\mathcal{M}(\oslash,\subseteq). \tag{13}$$

$$\mathcal{A}[Res_\kappa(\alpha,\theta)] = \aleph_\kappa(\alpha,\theta) - \frac{\vartheta_0(\alpha)}{\theta^2} - \frac{1}{\theta^{\hbar}}\mathcal{M}(\oslash,\subseteq). \tag{14}$$

Step 7. Use the expansion form of $\aleph_\kappa(\alpha,\theta)$ in $\mathcal{A}[Res_\kappa(\alpha,\theta)]$.
Step 8. Multiply both sides of $\mathcal{A}[Res_\kappa(\alpha,\theta)]$ by $\theta^{\kappa\hbar+2}$.
Step 9. By utilizing the fact in Equation (14), solve the following sequence of algebraic equations for $\vartheta_\nu(\alpha)$ step by step, where $\nu = 1,\ 2,\ 3, ...,\ \kappa$.

$$\lim_{\theta\to\infty}\left(\theta^{\kappa\hbar+2}\mathcal{A}[Res_\kappa(\alpha,\theta)]\right) = 0,\ \kappa = 1,\ 2,\ 3,\ ....\tag{15}$$

Step 10. Use the obtained values of $\vartheta_\nu(\alpha)$ in the κth truncated expansion of $\aleph(\alpha,\theta)$ for each $\nu = 1,\ 2,\ 3, ...,\ \kappa$ to attain the κth approximate solution of the algebraic equation in Equation (9).
Step 11. Apply $\mathcal{A}^{-1}$ on the final form of $\aleph_\kappa(\alpha,\theta)$ to obtain the κth approximate solution $\Omega_\kappa(\alpha,\tau)$ of the suggested problem.

4. Applications to Time-Fractional BSDEs

This section presents three problems to demonstrate the superiority and viability of the recommended approach for dealing with the time-fractional BSDEs. In our computational process, we used Mathematica 11 and Maple 2018.

Problem 1. *Consider the following time-fractional BS model [44]:*

$$\frac{\partial^{\hbar}\Omega(\alpha,\tau)}{\partial\tau^{\hbar}} + \alpha^2\frac{\partial^2\Omega(\alpha,\tau)}{\partial\alpha^2} + (0.5)\alpha\frac{\partial\Omega(\alpha,\tau)}{\partial\alpha} - \Omega(\alpha,\tau) = 0,\ 0 < \hbar \le 1, \tag{16}$$

with the preliminary conditions as follows:

$$\Omega(\alpha,0) = max(\alpha^3,0) = \begin{cases} \alpha^3 & for\ \alpha > 0, \\ 0 & for\ \alpha \le 0. \end{cases} \tag{17}$$

When we implement $\mathcal{A}$ on both sides of Equation (16), this yields

$$\mathcal{A}\Big[\frac{\partial^{\hbar}\Omega(\alpha,\tau)}{\partial\tau^{\hbar}}+\alpha^{2}\frac{\partial^{2}\Omega(\alpha,\tau)}{\partial\alpha^{2}}+(0.5)\alpha\frac{\partial\Omega(\alpha,\tau)}{\partial\alpha}-\Omega(\alpha,\tau)=0\Big]=0. \tag{18}$$

Using the methodology listed in Section 3, the following conclusions are drawn from Equation (18):

$$\aleph(\alpha,\theta)=\frac{\alpha^{3}}{\theta^{2}}-\frac{1}{\theta^{\hbar}}\alpha^{2}D_{\alpha\alpha}\mathcal{A}[\Omega(\alpha,\tau)]-\frac{1}{\theta^{\hbar}}(0.5)\alpha D_{\alpha}\mathcal{A}[\Omega(\alpha,\tau)]+\frac{1}{\theta^{\hbar}}\mathcal{A}[\Omega(\alpha,\tau)],\ \alpha>0. \tag{19}$$

We postulated that $\aleph(\alpha,\theta)$ expands to the following:

$$\aleph(\alpha,\theta)=\sum_{\nu=0}^{\infty}\frac{\vartheta_{\nu}(\alpha)}{\theta^{\nu\hbar+2}}. \tag{20}$$

$\aleph_{\kappa}(\alpha,\theta)$ is as follows:

$$\aleph_{\kappa}(\alpha,\theta)=\sum_{\nu=0}^{\kappa}\frac{\vartheta_{\nu}(\alpha)}{\theta^{\nu\hbar+2}}. \tag{21}$$

As a result of utilizing Lemma 1(iii), we determined the following:

$$\vartheta_{0}(\alpha)=\lim_{\theta\to\infty}\theta^{2}\aleph(\theta)=\Omega(\alpha,0)=\alpha^{3}.$$

As a result, the $\aleph_{\kappa}(\alpha,\theta)$ of Equation (19) is as follows:

$$\aleph_{\kappa}(\alpha,\theta)=\frac{\alpha^{3}}{\theta^{2}}+\sum_{\nu=1}^{\kappa}\frac{\vartheta_{\nu}(\alpha)}{\theta^{\nu\hbar+2}}. \tag{22}$$

We utilized the RPSM's feature to establish the following $\mathcal{ARF}$ of Equation (19) [50–52]:

$$\mathcal{A}[Res(\alpha,\theta)]=\aleph(\alpha,\theta)-\frac{\alpha^{3}}{\theta^{2}}+\frac{1}{\theta^{\hbar}}\alpha^{2}D_{\alpha\alpha}\aleph(\alpha,\theta)+\frac{1}{\theta^{\hbar}}(0.5)\alpha D_{\alpha}\aleph(\alpha,\theta)-\frac{1}{\theta^{\hbar}}\aleph(\alpha,\theta). \tag{23}$$

The following is the κth $\mathcal{ARF}$ of Equation (19):

$$\mathcal{A}[Res_{\kappa}(\alpha,\theta)]=\aleph_{\kappa}(\alpha,\theta)-\frac{\alpha^{3}}{\theta^{2}}+\frac{1}{\theta^{\hbar}}\alpha^{2}D_{\alpha\alpha}\aleph_{\kappa}(\alpha,\theta)+\frac{1}{\theta^{\hbar}}(0.5)\alpha D_{\alpha}\aleph_{\kappa}(\alpha,\theta)-\frac{1}{\theta^{\hbar}}\aleph_{\kappa}(\alpha,\theta). \tag{24}$$

We enhanced the RPSM's features to emphasize the following specifics [50–52]:

(i) $\mathcal{A}[Res(\alpha,\theta)]=0$ *and* $\lim_{\kappa\to\infty}\mathcal{A}[Res_{\kappa}(\alpha,\theta)]$;

(ii) $\lim_{\theta\to\infty}\theta^{2}\mathcal{A}[Res(\alpha,\theta)]=0\implies\lim_{\theta\to\infty}\theta^{2}\mathcal{A}[Res_{\kappa}(\alpha,\theta)]=0$;

(iii) $\lim_{\theta\to\infty}\theta^{\kappa\hbar+2}\mathcal{A}[Res(\alpha,\theta)]=\lim_{\theta\to\infty}\theta^{\kappa\hbar+2}\mathcal{A}[Res_{\kappa}(\alpha,\theta)]=0$.

where $\kappa=1,2,3,\ldots$ To determine the first unknown co-efficient $\vartheta_{1}(\alpha)$ in Equation (22), we have to use the first truncated series $\aleph_{1}(\alpha,\theta)=\frac{\alpha^{3}}{\theta^{2}}+\frac{\vartheta_{1}(\alpha)}{\theta^{\hbar+2}}$ in the first $\mathcal{ARF}$ $\mathcal{A}[Res_{1}(\alpha,\theta)]$ to obtain

$$\begin{aligned}\mathcal{A}[Res_{1}(\alpha,\theta)]=&\Big[\frac{\alpha^{3}}{\theta^{2}}+\frac{\vartheta_{1}(\alpha)}{\theta^{\hbar+2}}\Big]-\frac{\alpha^{3}}{\theta^{2}}+\frac{1}{\theta^{\hbar}}\alpha^{2}D_{\alpha\alpha}\Big[\frac{\alpha^{3}}{\theta^{2}}+\frac{\vartheta_{1}(\alpha)}{\theta^{\hbar+2}}\Big]+\\&\frac{1}{\theta^{\hbar}}(0.5)\alpha D_{\alpha}\Big[\frac{\alpha^{3}}{\theta^{2}}+\frac{\vartheta_{1}(\alpha)}{\theta^{\hbar+2}}\Big]-\frac{1}{\theta^{\hbar}}\Big[\frac{\alpha^{3}}{\theta^{2}}+\frac{\vartheta_{1}(\alpha)}{\theta^{\hbar+2}}\Big].\end{aligned} \tag{25}$$

$\theta^{\hbar+2}$ is used on both sides of Equation (25).

$$\begin{aligned}\theta^{\hbar+2}\mathcal{A}[Res_{1}(\alpha,\theta)]=&\vartheta_{1}(\alpha)+\alpha^{2}D_{\alpha\alpha}\Big[\alpha^{3}+\frac{\vartheta_{1}(\alpha)}{\theta^{\hbar}}\Big]+(0.5)\alpha D_{\alpha}\Big[\alpha^{3}+\frac{\vartheta_{1}(\alpha)}{\theta^{\hbar}}\Big]-\\&\Big[\alpha^{3}+\frac{\vartheta_{1}(\alpha)}{\theta^{\hbar}}\Big].\end{aligned} \tag{26}$$

Use the fact that:

$$\lim_{\theta\to\infty}\theta^{\kappa\hbar+2}\mathcal{A}[Res_{\kappa}(\alpha,\theta)]=0,\ for\ \kappa=1. \tag{27}$$

As a result, we obtain the following:

$$\vartheta_1(\alpha)=-6.5\alpha^3.$$

Similarly, to find the values of the second undefined co-efficient $\vartheta_2(\alpha)$*, we have to use the second truncated series:* $\aleph_2(\alpha,\theta)=\frac{\alpha^3}{\theta}+\frac{\vartheta_1(\alpha)}{\theta^{\hbar+2}}+\frac{\vartheta_2(\alpha)}{\theta^{2\hbar+2}}$ *in the second* $\mathcal{ARF}$ $\mathcal{A}[Res_2(\alpha,\theta)]$ *to obtain*

$$\begin{aligned}\mathcal{A}[Res_2(\alpha,\theta)]=&\Big[\frac{\alpha^3}{\theta^2}+\frac{\vartheta_1(\alpha)}{\theta^{\hbar+2}}+\frac{\vartheta_2(\alpha)}{\theta^{2\hbar+2}}\Big]-\frac{\alpha^3}{\theta^2}+\frac{1}{\theta^{\hbar}}\alpha^2D_{\alpha\alpha}\Big[\frac{\alpha^3}{\theta^2}+\frac{\vartheta_1(\alpha)}{\theta^{\hbar+2}}+\frac{\vartheta_2(\alpha)}{\theta^{2\hbar+2}}\Big]+\\&\frac{1}{\theta^{\hbar}}(0.5)\alpha D_{\alpha}\Big[\frac{\alpha^3}{\theta^2}+\frac{\vartheta_1(\alpha)}{\theta^{\hbar+2}}+\frac{\vartheta_2(\alpha)}{\theta^{2\hbar+2}}\Big]-\frac{1}{\theta^{\hbar}}\Big[\frac{\alpha^3}{\theta^2}+\frac{\vartheta_1(\alpha)}{\theta^{\hbar+2}}+\frac{\vartheta_2(\alpha)}{\theta^{2\hbar+2}}\Big].\end{aligned} \tag{28}$$

Using $\theta^{2\hbar+2}$ *on both sides of Equation* (28)*, we obtain the following:*

$$\begin{aligned}\theta^{2\hbar+2}\mathcal{A}[Res_2(\alpha,\theta)]=&\theta^{\hbar}\vartheta_1(\alpha)+\vartheta_2(\alpha)+\theta^{\hbar+2}\alpha^2D_{\alpha\alpha}\Big[\frac{\alpha^3}{\theta^2}+\frac{\vartheta_1(\alpha)}{\theta^{\hbar+2}}+\frac{\vartheta_2(\alpha)}{\theta^{2\hbar+2}}\Big]+\\&\theta^{\hbar+2}(0.5)D_{\alpha}\Big[\frac{\alpha^3}{\theta^2}+\frac{\vartheta_1(\alpha)}{\theta^{\hbar+2}}+\frac{\vartheta_2(\alpha)}{\theta^{2\hbar+2}}\Big]-\theta^{\hbar+2}\Big[\frac{\alpha^3}{\theta^2}+\frac{\vartheta_1(\alpha)}{\theta^{\hbar+2}}+\frac{\vartheta_2(\alpha)}{\theta^{2\hbar+2}}\Big].\end{aligned} \tag{29}$$

Again, use the fact that:

$$\lim_{\theta\to\infty}\theta^{\kappa\hbar+2}\mathcal{A}[Res_{\kappa}(\alpha,\theta)]=0,\ for\ \kappa=2. \tag{30}$$

As a result, we obtained the second coefficient $\vartheta_2(\alpha)$ *in the following form:*

$$\vartheta_2(\alpha)=(6.5)^2\alpha^3.$$

Therefore, the second approximate ARPS solution of Equation (19) *is*

$$\aleph_2(\alpha,\theta)=\frac{1}{\theta^2}\alpha^3-\frac{6.5}{\theta^{\hbar+2}}\alpha^3+\frac{(6.5)^2}{\theta^{2\hbar+2}}\alpha^3. \tag{31}$$

Typically, to find the coefficients $\vartheta_\kappa(\alpha)$*, first use the* κ*th truncated series in Equation* (22)*, then utilize it in the* κ*th* $\mathcal{ARF}$*, Equation* (24)*, multiply* $\mathcal{A}[Res_\kappa(\alpha,\theta)]$ *by* $\theta^{\kappa\hbar+2}$*, then solve the algebraic equation below.*

$$\lim_{\theta\to\infty}\theta^{\kappa\hbar+2}\mathcal{A}[Res_{\kappa}(\alpha,\theta)]=0,\ for\ \vartheta_\kappa(\alpha).$$

We obtain the following results by utilizing the above procedure:

$$\begin{aligned}\vartheta_3(\alpha)=&-(6.5)^3\alpha^3.\\\vartheta_4(\alpha)=&(6.5)^4\alpha^3.\\\vartheta_5(\alpha)=&-(6.5)^5\alpha^3.\end{aligned}$$

The approximate solution of Equation (19) *is obtained by five iterations as follows:*

$$\aleph_5(\alpha,\theta)=\frac{\alpha^3}{\theta^2}-\frac{6.5\alpha^3}{\theta^{\hbar+2}}+\frac{(6.5)^2\alpha^3}{\theta^{2\hbar+2}}-\frac{(6.5)^3\alpha^3}{\theta^{3\hbar+2}}+\frac{(6.5)^4\alpha^3}{\theta^{4\hbar+2}}-\frac{(6.5)^5\alpha^3}{\theta^{5\hbar+2}}. \tag{32}$$

By applying $\mathcal{A}^{-1}$ *to Equation* (32)*, we are able to approximate the fifth step solution in the original feature space.*

$$\Omega_5(\alpha,\tau) = \alpha^3 - \frac{6.5\alpha^3\tau^{\hbar}}{\Gamma(\hbar+1)} + \frac{(6.5)^2\alpha^3\tau^{2\hbar}}{\Gamma(2\hbar+1)} - \frac{(6.5)^3\alpha^3\tau^{3\hbar}}{\Gamma(3\hbar+1)} + \frac{(6.5)^4\alpha^3\tau^{4\hbar}}{\Gamma(4\hbar+1)} - \frac{(6.5)^5\alpha^3\tau^{5\hbar}}{\Gamma(5\hbar+1)}. \quad (33)$$

When we use $\hbar = 1.0$ *in Equation* (33)*, we obtain the following form:*

$$\Omega_5(\alpha,\tau) = \alpha^3\left[1 + \frac{(-6.5\tau)}{1!} + \frac{(-6.5\tau)^2}{2!} + \frac{(-6.5\tau)^3}{3!} + \frac{(-6.5\tau)^4}{4!} + \frac{(-6.5\tau)^5}{5!}\right]. \quad (34)$$

This comprises the first six terms of the expansion $\alpha^3 e^{-6.5\tau}$ *and, thus, is the exact solution of Equations* (16) *and* (17) *at* $\hbar = 1.0$*.*

Problem 2. *Take into account the subsequent time-fractional BS model [45]:*

$$\frac{\partial^{\hbar}\Omega(\alpha,\tau)}{\partial\tau^{\hbar}} + 0.08(2+sin\alpha)^2\alpha^2\frac{\partial^2\Omega(\alpha,\tau)}{\partial\alpha^2} + 0.06\alpha\frac{\partial\Omega(\alpha,\tau)}{\partial\alpha} = 0.06\Omega(\alpha,\tau),\ 0 < \hbar \leq 1, \quad (35)$$

subject to the following initial conditions:

$$\Omega(\alpha,0) = max(\alpha - 25e^{-0.06}, 0). \quad (36)$$

First, perform $\mathcal{A}$ *on both sides of Equation* (35)*, using the initial condition from Equation* (36)*, and then, format the resulting equation as follows:*

$$\begin{aligned}\aleph(\alpha,\theta) =& \frac{1}{\theta^2}max(\alpha - 25e^{-0.06}, 0) - \frac{1}{\theta^{\hbar}}0.08(2+sin\alpha)^2\alpha^2 D_{\alpha\alpha}\aleph(\alpha,\theta) - \\ & \frac{0.06\alpha}{\theta^{\hbar}}D_{\alpha}\aleph(\alpha,\theta) + \frac{0.06}{\theta^{\hbar}}\aleph(\alpha,\theta). \end{aligned} \quad (37)$$

Describe the expansion solution of the algebraic equation Equation (37)*. Therefore, we suppose that the series of* $\aleph(\alpha,\theta)$ *is as follows:*

$$\aleph(\alpha,\theta) = \sum_{\nu=0}^{\infty}\frac{\vartheta_{\nu}(\alpha)}{\theta^{\nu\hbar+2}}. \quad (38)$$

The κ*th truncated series of the expansion of* $\aleph(\alpha,\theta)$ *is:*

$$\aleph_{\kappa}(\alpha,\theta) = \sum_{\nu=0}^{\kappa}\frac{\vartheta_{\nu}(\alpha)}{\theta^{\nu\hbar+2}}. \quad (39)$$

We obtained the following as a result of using Lemma 1(iii).

$$\vartheta_0(\alpha) = \lim_{\theta\to\infty}\theta^2\aleph(\alpha,\theta) = \Omega(\alpha,0) = max(\alpha - 25e^{-0.06}, 0). \quad (40)$$

Therefore, the κ*th truncated expansion becomes:*

$$\aleph_{\kappa}(\alpha,\theta) = \frac{1}{\theta^2}max(\alpha - 25e^{-0.06}, 0) + \sum_{\nu=1}^{\kappa}\frac{\vartheta_{\nu}(\alpha)}{\theta^{\nu\hbar+2}}. \quad (41)$$

The $\mathcal{ARF}$ *of Equation* (37) *is as follows:*

$$\begin{aligned}\mathcal{A}[Res(\alpha,\theta)] =& \aleph(\alpha,\theta) - \frac{1}{\theta^2}max(\alpha - 25e^{-0.06}, 0) + \frac{1}{\theta^{\hbar}}0.08(2+sin\alpha)^2\alpha^2 D_{\alpha\alpha}\aleph(\alpha,\theta) \\ & + \frac{0.06\alpha}{\theta^{\hbar}}D_{\alpha}\aleph(\alpha,\theta) - \frac{0.06}{\theta^{\hbar}}\aleph(\alpha,\theta). \end{aligned} \quad (42)$$

The κth $\mathcal{ARF}$ of Equation (37) is designed as follows:

$$\begin{aligned}\mathcal{A}[Res_\kappa(\alpha,\theta)] =&\aleph_\kappa(\alpha,\theta) - \frac{1}{\theta^2}max(\alpha - 25e^{-0.06},0) + \frac{1}{\theta^{\hbar}}0.08(2+sin\alpha)^2\alpha^2 D_{\alpha\alpha}\aleph_\kappa(\alpha,\theta)\\ &+ \frac{0.06\alpha}{\theta^{\hbar}}D_\alpha\aleph_\kappa(\alpha,\theta) - \frac{0.06}{\theta^{\hbar}}\aleph_\kappa(\alpha,\theta).\end{aligned} \tag{43}$$

To determine the first unknown coefficient $\vartheta_1(\alpha)$ in Equation (39), we have to use the first truncated expansion $\aleph_1(\alpha,\theta) = \frac{1}{\theta^2}\max(\alpha - 25e^{-0.06},0) + \frac{\vartheta_1(\alpha)}{\theta^{\hbar+2}}$ in the first $\mathcal{ARF}$ $\mathcal{A}[Res_1(\alpha,\theta)]$, then multiply by $\theta^{\hbar+2}$ on both sides, then use the following fact $\lim_{\theta\to\infty}\theta^{\hbar+2}\mathcal{A}[Res_1(\alpha,\theta)] = 0$ to obtain

$$\vartheta_1(\alpha) = -0.06[\alpha - \max(\alpha - 25e^{-0.06},0)].$$

Similarly, to establish the value of the second undefined coefficient $\vartheta_2(\alpha)$, we have to utilize the second truncated expansion $\aleph_2(\alpha,\theta) = \frac{1}{\theta^2}\max(\alpha - 25e^{-0.06},0) + \frac{\vartheta_1(\alpha)}{\theta^{\hbar+2}} + \frac{\vartheta_2(\alpha)}{\theta^{2\hbar+2}}$ in the second $\mathcal{ARF}$ and use the following fact $\lim_{\theta\to\infty}\theta^{2\hbar+2}\mathcal{A}[Res_2(\alpha,\theta)] = 0$, then we have

$$\vartheta_2(\alpha) = -(0.06)^2(\alpha - \max(\alpha - 25e^{-0.06},0).$$

Therefore, the approximate solution derived from the second iteration of Equation (37) is as follows:

$$\begin{aligned}\aleph_2(\alpha,\theta) =&\frac{1}{\theta^2}(\max(\alpha - 25e^{-0.06},0)) - \frac{0.06}{\theta^{\hbar+2}}(\alpha - \max(\alpha - 25e^{-0.06},0)) -\\ &\frac{(0.06)^2}{\theta^{2\hbar+2}}(\alpha - \max(\alpha - 25e^{-0.06},0)).\end{aligned} \tag{44}$$

To determine the 3rd, 4th, and 5th unknown coefficients, repeat the same process. We obtain:

$$\begin{aligned}\vartheta_3(\alpha) &= -(0.06)^3(\alpha - \max(\alpha - 25e^{-0.06},0)).\\ \vartheta_4(\alpha) &= -(0.06)^4(\alpha - \max(\alpha - 25e^{-0.06},0)).\\ \vartheta_5(\alpha) &= -(0.06)^5(\alpha - \max(\alpha - 25e^{-0.06},0)).\end{aligned}$$

Therefore, the approximate solution derived from the fifth iteration of Equation (37) is as follows:

$$\begin{aligned}\aleph_5(\alpha,\theta) =&\frac{1}{\theta^2}(\max(\alpha - 25e^{-0.06},0)) - \Big[\frac{0.06}{\theta^{\hbar+2}} + \frac{(0.06)^2}{\theta^{2\hbar+2}} + \frac{(0.06)^3}{\theta^{3\hbar+2}} + \frac{(0.06)^4}{\theta^{4\hbar+2}} +\\ &\frac{(0.06)^5}{\theta^{5\hbar+2}}\Big](\alpha - \max(\alpha - 25e^{-0.06},0)).\end{aligned} \tag{45}$$

By utilizing $\mathcal{A}^{-1}$ on both sides of Equation (45), the approximate solution derived from the fifth iteration by the ARPSM of Equations (35) and (36) is as follows:

$$\begin{aligned}\Omega_5(\alpha,\tau) =&max(\alpha - 25e^{-0.06},0) - \Big[\frac{(0.06\tau^{\hbar})}{\Gamma(\hbar+1)} + \frac{(0.06\tau^{\hbar})^2}{\Gamma(2\hbar+1)} + \frac{(0.06\tau^{\hbar})^3}{\Gamma(3\hbar+1)} + \frac{(0.06\tau^{\hbar})^4}{\Gamma(4\hbar+2)} +\\ &\frac{(0.06\tau^{\hbar})^5}{\Gamma(5\hbar+1)}\Big](\alpha - \max(\alpha - 25e^{-0.06},0)).\end{aligned} \tag{46}$$

When $\hbar = 1.0$ is used in Equation (46), we obtain:

$$\begin{aligned}\Omega_5(\alpha,\tau) =&\max(\alpha - 25e^{-0.06},0) - \Big[0.06\tau + \frac{(0.06\tau)^2}{2!} + \frac{(0.06\tau)^3}{3!} + \frac{(0.06\tau)^4}{4!} +\\ &\frac{(0.06\tau)^5}{5!}\Big](\alpha - \max(\alpha - 25e^{-0.06},0)).\end{aligned} \tag{47}$$

As a result, the following is the exact solution of Equations (35) and (36) for $\hbar = 1.0$.

$$\Omega(\alpha,\tau) = \max(\alpha - 25e^{-0.06}, 0) + (1 - e^{0.06\tau})(\alpha - \max(\alpha - 25e^{-0.06}, 0)).$$

Problem 3. *Consider the following time-fractional BS model [46]:*

$$\frac{\partial^{\hbar}\Omega(\alpha,\tau)}{\partial\tau^{\hbar}} = \frac{\partial^2\Omega(\alpha,\tau)}{\partial\alpha^2} + (\xi - 1)\frac{\partial\Omega(\alpha,\tau)}{\partial\alpha} - \xi\Omega(\alpha,\tau),\ 0 < \hbar \leq 1, \tag{48}$$

subject to the initial condition:

$$\Omega(\alpha, 0) = \max(e^{\hbar} - 1, 0). \tag{49}$$

First, perform $\mathcal{A}$ *on both sides of Equation (48), using the initial condition from Equation (49), and then, format the resulting equation as follows:*

$$\aleph(\alpha,\theta) = \frac{1}{\theta^2}\max(e^{\alpha} - 1, 0) + \frac{1}{\theta^{\hbar}}D_{\alpha\alpha}\aleph(\alpha,\theta) + \frac{(\xi - 1)}{\theta^{\hbar}}D_{\alpha}\aleph(\alpha,\theta) - \frac{\xi}{\theta^{\hbar}}\aleph(\alpha,\theta). \tag{50}$$

Describe the expansion solution of the algebraic Equation (50). Therefore, we assumed that the expansion of $\aleph(\alpha,\theta)$ *is as follows:*

$$\aleph(\alpha,\theta) = \sum_{\nu=0}^{\infty}\frac{\vartheta_{\nu}(\alpha)}{\theta^{\nu\hbar+2}}. \tag{51}$$

The κ*th truncated expansion of Equation (50) is as follows:*

$$\aleph_{\kappa}(\alpha,\theta) = \frac{1}{\theta^2}\max(e^{\alpha} - 1, 0) + \sum_{\nu=1}^{\kappa}\frac{\vartheta_{\nu}(\alpha)}{\theta^{\nu\hbar+2}}. \tag{52}$$

The $\mathcal{ARF}$ *of Equation (50) takes the following form:*

$$\begin{aligned}\mathcal{A}[Res(\alpha,\theta)] =& \aleph(\alpha,\theta) - \frac{1}{\theta^2}\max(e^{\alpha} - 1, 0) - \frac{1}{\theta^{\hbar}}D_{\alpha\alpha}\aleph(\alpha,\theta) - \frac{(\xi - 1)}{\theta^{\hbar}}D_{\alpha}\aleph(\alpha,\theta) + \\ & \frac{\xi}{\theta^{\hbar}}\aleph(\alpha,\theta).\end{aligned} \tag{53}$$

Accordingly, the κ*th* $\mathcal{ARF}$ *takes the form:*

$$\begin{aligned}\mathcal{A}[Res_{\kappa}(\alpha,\theta)] =& \aleph_{\kappa}(\alpha,\theta) - \frac{1}{\theta^2}\max(e^{\alpha} - 1, 0) - \frac{1}{\theta^{\hbar}}D_{\alpha\alpha}\aleph_{\kappa}(\alpha,\theta) - \frac{(\xi - 1)}{\theta^{\hbar}}D_{\alpha}\aleph_{\kappa}(\alpha,\theta) + \\ & \frac{\xi}{\theta^{\hbar}}\aleph_{\kappa}(\alpha,\theta).\end{aligned} \tag{54}$$

Substitute the κ*th truncated series Equation (52) into (53), multiply the resulting equation by* $\theta^{\kappa\hbar+2}$*, and then, solve the equation* $\lim_{\theta\to\infty}\theta^{\kappa\hbar+2}\mathcal{A}[Res_{\kappa}(\alpha,\theta)] = 0$*, where* $\kappa = 1, 2, 3, 4, 5$*, for* $\vartheta_{\kappa}(\alpha)$ *gives*

$$\begin{aligned}\vartheta_0(\alpha,\theta) =& max(e^{\alpha} - 1, 0).\\ \vartheta_1(\alpha,\theta) =& \xi[\max(e^{\alpha}, 0) - \max(e^{\alpha} - 1, 0)].\\ \vartheta_2(\alpha,\theta) =& -\xi^2[\max(e^{\alpha}, 0) - \max(e^{\alpha} - 1, 0)].\\ \vartheta_3(\alpha,\theta) =& \xi^3[\max(e^{\alpha}, 0) - \max(e^{\alpha} - 1, 0)].\\ \vartheta_4(\alpha,\theta) =& -\xi^4[\max(e^{\alpha}, 0) - \max(e^{\alpha} - 1, 0)].\\ \vartheta_5(\alpha,\theta) =& \xi^5[\max(e^{\alpha}, 0) - \max(e^{\alpha} - 1, 0)].\end{aligned}$$

Therefore, the approximate solution derived from the fifth iteration of Equation (50) is as follows:

$$\begin{aligned}\aleph_5(\alpha,\theta) =& \frac{1}{\theta^2}\max(e^{\alpha}-1,0)+\frac{\xi}{\theta^{\hbar+2}}[\max(e^{\alpha},0)-\max(e^{\alpha}-1,0)]-\frac{\xi^2}{\theta^{2\hbar+2}}[\max(e^{\alpha},0)-\\ &\max(e^{\alpha}-1,0)]+\frac{\xi^3}{\theta^{3\hbar+2}}[max(e^{\alpha},0)-\max(e^{\alpha}-1,0)]-\frac{\xi^4}{\theta^{4\hbar+2}}[\max(e^{\alpha},0)-\\ &\max(e^{\alpha}-1,0)]+\frac{\xi^5}{\theta^{5\hbar+2}}[\max(e^{\hbar},0)-\max(e^{\hbar}-1,0)]. \end{aligned} \tag{55}$$

By utilizing the $\mathcal{A}^{-1}$ on both sides of Equation (55), the approximate solution derived from the fifth iteration by the ARPSM of Equations (48) and (49) is as follows:

$$\begin{aligned}\Omega_5(\alpha,\tau) =& \max(e^{\alpha}-1,0)+\frac{\xi\tau^{\hbar}}{\Gamma(\hbar+1)}[\max(e^{\alpha},0)-\max(e^{\alpha}-1,0)]-\frac{\xi^2\tau^{2\hbar}}{\Gamma(2\hbar+1)}\\ &[\max(e^{\alpha},0)-\max(e^{\alpha}-1,0)]+\frac{\xi^3\tau^{3\hbar}}{\Gamma(3\hbar+1)}[\max(e^{\alpha},0)-\max(e^{\alpha}-1,0)]-\\ &\frac{\xi^4\tau^{4\hbar}}{\Gamma(4\hbar+1)}[\max(e^{\alpha},0)-\max(e^{\alpha}-1,0)]+\frac{\xi^5\tau^{5\hbar}}{\Gamma(5\hbar+1)}[\max(e^{\alpha},0)-\max(e^{\alpha}-1,0)]. \end{aligned} \tag{56}$$

When $\hbar = 1.0$ is used in Equation (56), we obtain:

$$\Omega_5(\alpha,\tau) = \max(e^{\alpha}-1,0)+\left[\frac{\xi\tau}{1!}-\frac{\xi^2\tau^2}{2!}+\frac{\xi^3\tau^3}{3!}-\frac{\xi^4\tau^4}{4!}+\frac{\xi^5\tau^5}{5!}\right][\max(e^{\alpha},0)-\max(e^{\alpha}-1,0)]. \tag{57}$$

As a result, the following is the exact solution of Equations (48) and (49) for $\hbar = 1.0$.

$$\Omega(\alpha,\tau) = \max(e^{\alpha}-1,0)e^{-\xi\tau}+\max(e^{\alpha},0)(1-e^{-\xi\tau}).$$

5. Numerical Simulation and Discussion

The findings of the results of the models presented in Problems 1–3 are evaluated graphically and numerically in this section. The correctness of the approximate numerical method can be assessed using an error function. It is crucial to express the error in terms of an infinite fractional power series of the approximate analytical solution that the ARPSM provides. We used the Abs. E and Rec. E functions to demonstrate the accuracy of the ARPSM. The Abs. E for the approximate κth step solution is determined as follows:

$$Abs.\ E^{\kappa}(\alpha,\tau) = |\Omega(\alpha,\tau)-\Omega^{\kappa}(\alpha,\tau)|,\ \kappa = 1,\ 2,\ 3,\cdots, \tag{58}$$

where Abs. $E^{\kappa}(\alpha,\tau)$ denotes the Abs. E for the κth step approximate solution. The Rec. E for the approximate κth step solution is determined as follows:

$$Rec\ E^{\kappa}(\alpha,\tau) = |\Omega^{\kappa+1}(\alpha,\tau)-\Omega^{\kappa}(\alpha,\tau)|,\ \kappa = 1,\ 2,\ 3,\cdots, \tag{59}$$

where Rec. $E^{\kappa}(\alpha,\tau)$ denotes the Rec. E for the κth step approximate solution. In fact, as κ approaches infinity, the Abs. $E^{\kappa}(\alpha,\tau)$ and Rec. $E^{\kappa}(\alpha,\tau)$ become smaller and smaller, approaching zero. Figure 1a–c show the 2D graphs of the comparative analysis of the exact and approximate solutions derived by the suggested method in Examples 1–3. These figures show the 2D plots of the exact and approximate solutions obtained by the ARPSM from the five iterations for Examples 1–3 when $\hbar = 0.6,\ 0.7,\ 0.8,\ 0.9$, and 1.0 in the $\tau \in [0,\ 0.5]$ range. These graphs show how the approximate solution converges to the exact solution when $\hbar \to 1.0$ is applied. At $\hbar = 1.0$, the exact and approximate solutions overlap, demonstrating the accuracy of the proposed method. For $\hbar = 1.0$ in the range of $\tau \in [0, 0.5]$, Figure 2a–c show the 2D curve of the Abs. E of the approximate solution established from the five steps and the exact solution found by the suggested technique. Figure 3a–c depict the comparison study using the 3D curve in terms of the Abs. E of the approximate finding from the five iterations and the exact finding using the suggested method for Problems 1–3

in the intervals $\tau \in [0, 0.2]$ and $\alpha \in [0, 0.2]$ at $\hbar = 1.0$, respectively. According to the study, the precise outcome and the proposed approach's fifth step approximation are very similar. The study demonstrates that the proposed approach's fifth step approximation solution is quite close to the exact solution. The precision of the ARPSM is demonstrated by plotting the Abs. E on a graph.

In Tables 1–9, the numerical convergence of the approximation to the exact solution is demonstrated by $| \Omega^4(\alpha, \tau) - \Omega^3(\alpha, \tau) |$, $| \Omega^5(\varkappa, \tau) - \Omega^4(\alpha, \tau) |$ and $| \Omega^6(\varkappa, \tau) - \Omega^5(\alpha, \tau) |$ in the range $\tau \in [0,\ 0.10]$. Tables 1–9 show that the $\Omega^4(\alpha, \tau)$ and $\Omega^5(\alpha, \tau)$ obtained by the ARPSM quickly approach $\Omega(\alpha, \tau)$ when $\hbar \to 1.0$. We can see from Tables 1, 4, and 7 that all of the test problems for the fourth stage have very low Rec. E. The Rec. E will further decrease if we take into account the fifth and sixth step approximations, as we can see from Tables 2, 3, 5, 6, 8, and 9. The approximation is rapidly approaching the exact solution as a result of the accuracy of our suggested strategy, demonstrated by the Rec. E process. We arrived at the conclusion that the suggested approach is a feasible and efficient technique for solving particular classes of FODEs with fewer calculations and iteration steps.

The $| \Omega(\alpha, \tau) - \Omega^5(\alpha, \tau) |$, $| \Omega(\alpha, \tau) - \Omega^6(\alpha, \tau) |$, and $| \Omega(\alpha, \tau) - \Omega^7(\alpha, \tau) |$ obtained by the ARPSM at $\hbar = 1.0$ for appropriately selected points are displayed in Tables 10–12 for a comparison study in the sense of the Abs.E of the approximate and exact finding. Tables 10–12 show that all of the approximations to the test problems that were created after five iterations have extremely low error rates. The Abs. E will continue to fall if the sixth and seventh step estimations are taken into consideration. By quantitatively contrasting the exact and approximative findings in the sense of the Abs. E, the accuracy of the ARPSM is shown.

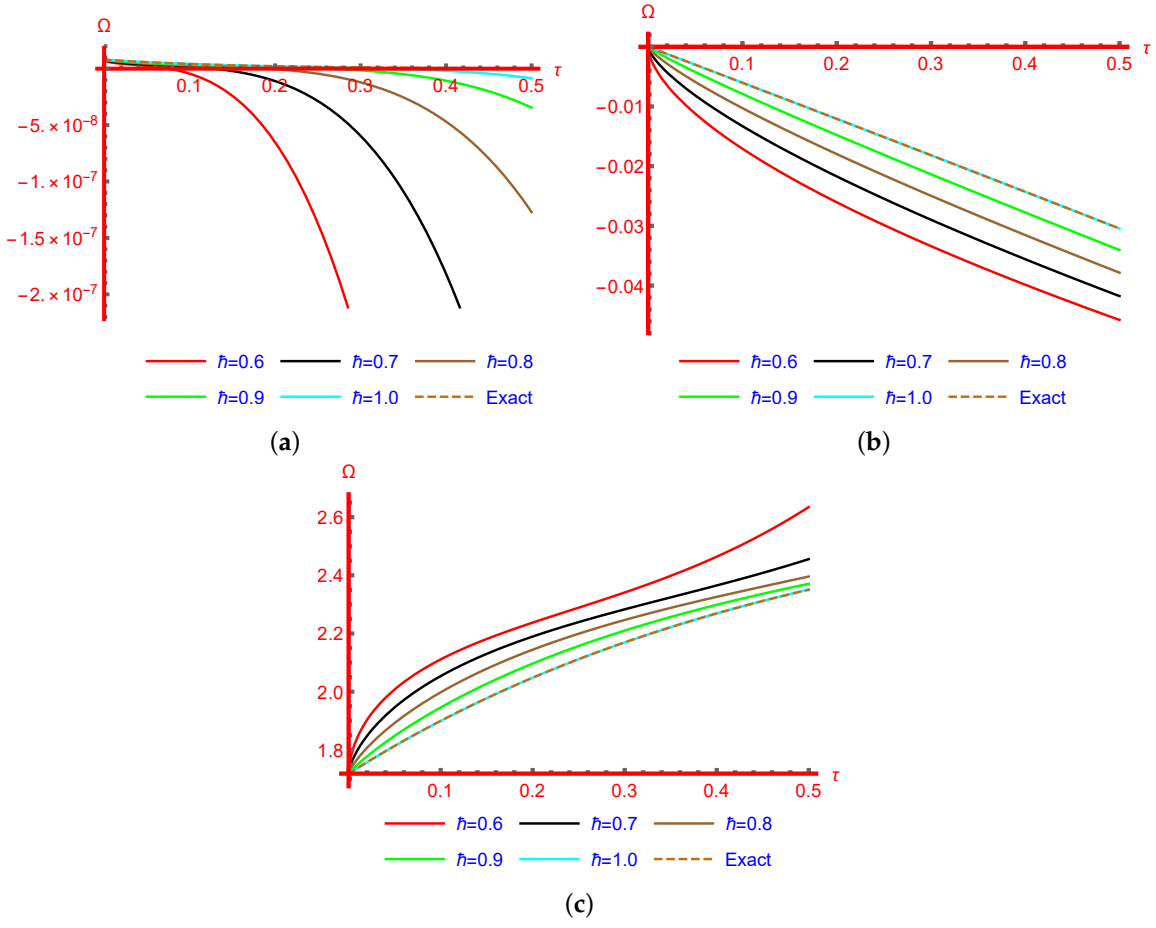

Figure 1. Figure 1 depicts the approximate result of five iterations, as well as the exact result of $\Omega(\alpha, \tau)$ for various values of $\hbar$ in the range $\tau \in [0,\ 0.5]$ for (**a**): Problem 1, when $\alpha = 0.002$; (**b**): Problem 2, when $\alpha = 1.0$; (**c**): Problem 3, when $\alpha = 1.0$ and $\xi = 2.0$.

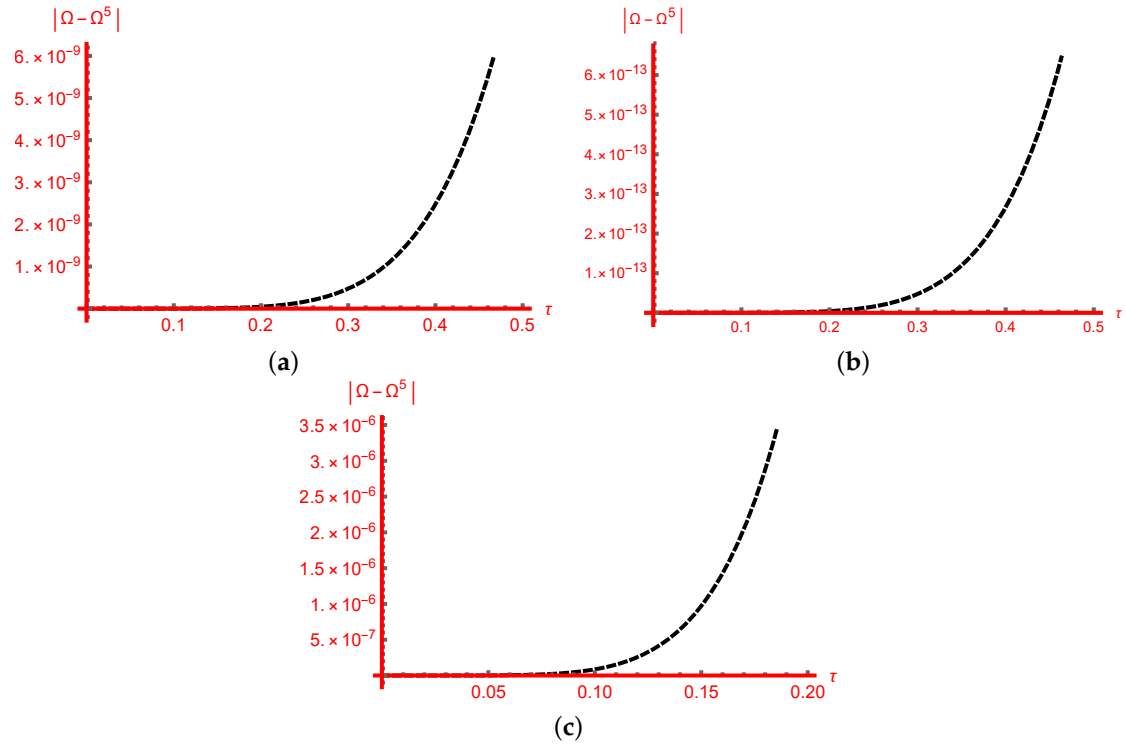

Figure 2. In Figure 2, the 2D curve of the $|\ \Omega(\alpha,\tau)-\Omega^5(\alpha,\tau)\ |$ in the range $\tau\in[0,\ 0.5]$, when $\hbar=1.0$ for (**a**): Problem 1, when $\alpha=0.002$; (**b**): Problem 2, when $\alpha=1.0$; (**c**): Problem 3,when $\alpha=1.0$ and $\xi=2.0$.

Table 1. The $|\ \Omega^4(\alpha,\tau)-\Omega^3(\alpha,\tau)\ |$ of Problem 1 at varying values of $\hbar$ at $\alpha=0.002$ determined by the ARPSM at plausible locations in the range $\tau\in[0,\ 0.10]$.

τ	$\hbar=0.7$	$\hbar=0.8$	$\hbar=0.9$	$\hbar=1.0$
0.01	7.64160×10^{-12}	7.32938×10^{-13}	6.73357×10^{-14}	5.95021×10^{-15}
0.02	5.32192×10^{-11}	6.73539×10^{-12}	8.16495×10^{-13}	9.52033×10^{-14}
0.03	1.65624×10^{-10}	2.46522×10^{-11}	3.51465×10^{-12}	4.81967×10^{-13}
0.04	3.70640×10^{-10}	6.18955×10^{-11}	9.90060×10^{-12}	1.52325×10^{-12}
0.05	6.92309×10^{-10}	1.26407×10^{-10}	2.21074×10^{-11}	3.71888×10^{-12}
0.06	1.15347×10^{-9}	2.26543×10^{-10}	4.26177×10^{-11}	7.71147×10^{-12}
0.07	1.77606×10^{-9}	3.71006×10^{-10}	7.42333×10^{-11}	1.42865×10^{-11}
0.08	2.58129×10^{-9}	5.68794×10^{-10}	1.20052×10^{-10}	2.43721×10^{-11}
0.09	3.58974×10^{-9}	8.29169×10^{-10}	1.83450×10^{-10}	3.90393×10^{-11}
0.10	4.82152×10^{-9}	1.84106×10^{-10}	3.37478×10^{-11}	5.95021×10^{-12}

Table 2. The $|\ \Omega^5(\alpha,\tau)-\Omega^4(\alpha,\tau)\ |$ of Problem 1 at varying values of $\hbar$ at $\alpha=0.002$ determined by the ARPSM at plausible locations in the range $\tau\in[0,\ 0.10]$.

τ	$\hbar=0.7$	$\hbar=0.8$	$\hbar=0.9$	$\hbar=1.0$
0.01	7.98018×10^{-13}	3.86764×10^{-14}	1.77337×10^{-15}	7.73527×10^{-17}
0.02	9.02854×10^{-12}	6.18822×10^{-13}	4.01268×10^{-14}	2.47529×10^{-15}
0.03	3.73196×10^{-11}	3.13278×10^{-12}	2.48797×10^{-13}	1.87967×10^{-14}
0.04	1.02146×10^{-10}	9.90115×10^{-12}	9.07967×10^{-13}	7.92092×10^{-14}
0.05	2.23053×10^{-10}	2.41727×10^{-11}	2.47836×10^{-12}	2.41727×10^{-13}
0.06	4.22223×10^{-10}	5.01246×10^{-11}	5.62964×10^{-12}	6.01495×10^{-13}
0.07	7.24195×10^{-10}	9.28619×10^{-11}	1.12653×10^{-11}	1.30007×10^{-12}
0.08	1.15565×10^{-9}	1.58418×10^{-10}	2.05449×10^{-11}	2.53469×10^{-12}
0.09	1.74526×10^{-9}	2.53756×10^{-10}	3.49053×10^{-11}	4.56760×10^{-12}
0.10	2.52355×10^{-9}	3.86764×10^{-10}	5.6079×10^{-11}	7.73527×10^{-12}

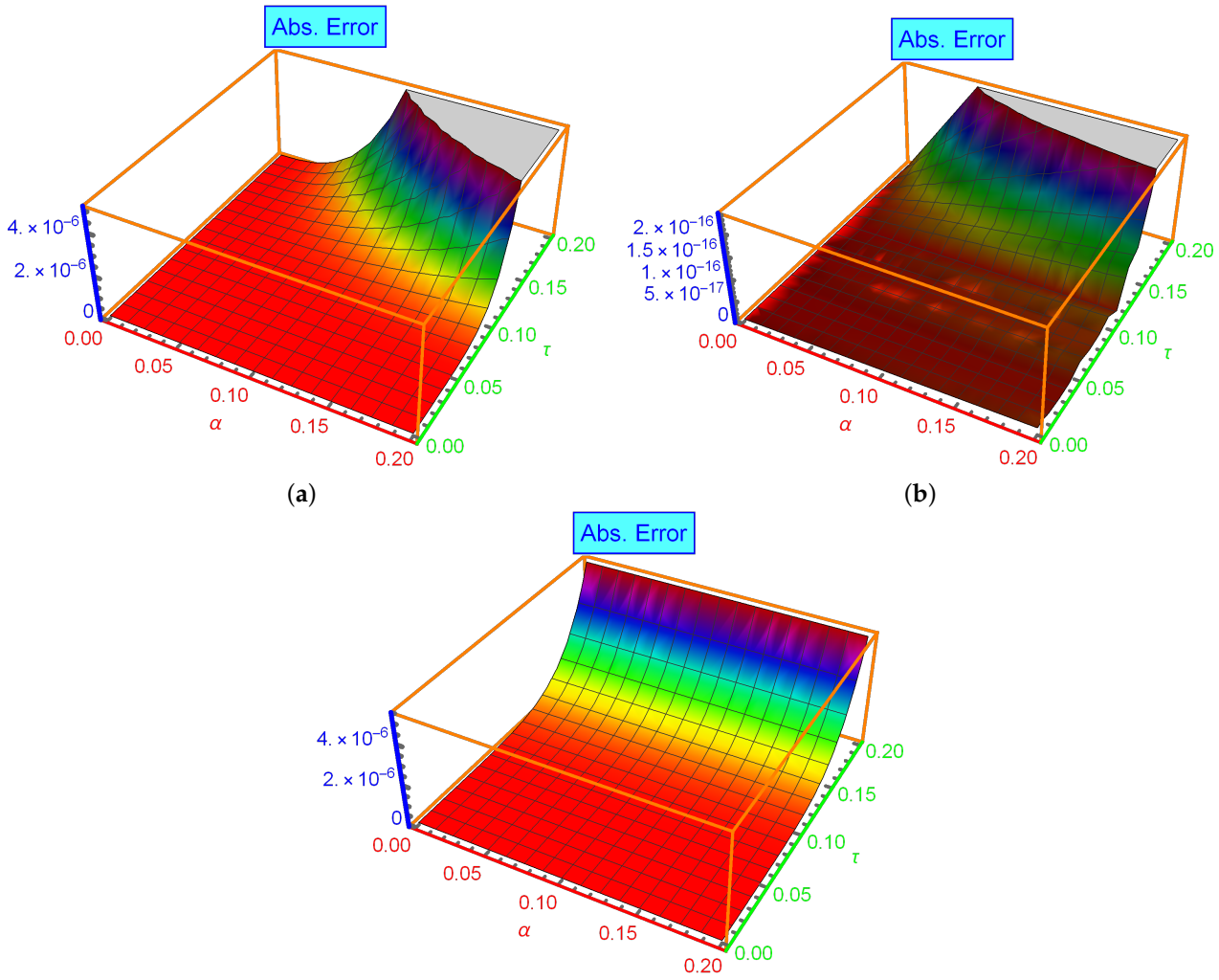

Figure 3. In Figure 3, the 3D curve of the $\mid \Omega(\alpha,\tau) - \Omega^5(\alpha,\tau) \mid$ in the ranges $\tau \in [0,\ 0.2]$ and $\alpha \in [0,\ 0.2]$, when $\hbar = 1.0$ for (**a**): Problem 1; (**b**): Problem 2; (**c**): Problem 3, when $\xi = 2.0$.

Table 3. The $\mid \Omega^6(\alpha,\tau) - \Omega^5(\alpha,\tau) \mid$ of Problem 1 at varying values of $\hbar$ at $\alpha = 0.002$ determined by the ARPSM at plausible locations in the range $\tau \in [0,\ 0.10]$.

τ	$\hbar = 0.7$	$\hbar = 0.8$	$\hbar = 0.9$	$\hbar = 1.0$
0.01	7.37300×10^{-14}	1.77005×10^{-15}	3.97057×10^{-17}	8.37988×10^{-19}
0.02	1.35510×10^{-12}	4.93094×10^{-14}	1.67654×10^{-15}	5.36312×10^{-17}
0.03	7.43967×10^{-12}	3.45277×10^{-13}	1.49730×10^{-14}	6.10893×10^{-16}
0.04	2.49056×10^{-11}	1.37364×10^{-12}	7.07908×10^{-14}	3.43240×10^{-15}
0.05	6.35797×10^{-11}	4.00906×10^{-12}	2.36206×10^{-13}	1.30936×10^{-14}
0.06	1.36735×10^{-10}	9.61861×10^{-12}	6.32222×10^{-13}	3.90972×10^{-14}
0.07	2.61250×10^{-10}	2.01584×10^{-11}	1.45339×10^{-12}	9.85884×10^{-14}
0.08	4.57744×10^{-10}	3.82664×10^{-11}	2.98909×10^{-12}	2.19673×10^{-13}
0.09	7.50694×10^{-10}	6.73519×10^{-11}	5.64628×10^{-12}	4.45341×10^{-13}
0.10	1.16854×10^{-9}	1.11683×10^{-10}	9.97362×10^{-12}	8.37988×10^{-13}

Table 4. The $|\ \Omega^4(\alpha,\tau)-\Omega^3(\alpha,\tau)\ |$ of Problem 2 at varying values of $\hbar$ at $\alpha=1.0$ determined by the ARPSM at plausible locations in the range $\tau\in[0,\ 0.10]$.

τ	$\hbar=0.7$	$\hbar=0.8$	$\hbar=0.9$	$\hbar=1.0$
0.01	6.93499×10^{-12}	6.65164×10^{-13}	6.11093×10^{-14}	5.40000×10^{-15}
0.02	4.82981×10^{-11}	6.11258×10^{-12}	7.40995×10^{-13}	8.64000×10^{-14}
0.03	1.50309×10^{-10}	2.23726×10^{-11}	3.18965×10^{-12}	4.37400×10^{-13}
0.04	3.36367×10^{-10}	5.61721×10^{-11}	8.98510×10^{-12}	1.38240×10^{-12}
0.05	6.28292×10^{-10}	1.14718×10^{-10}	2.00632×10^{-11}	3.37500×10^{-12}
0.06	1.04681×10^{-9}	2.05595×10^{-10}	3.86769×10^{-11}	6.99840×10^{-12}
0.07	1.61183×10^{-9}	3.36699×10^{-10}	6.73690×10^{-11}	1.29654×10^{-11}
0.08	2.34260×10^{-9}	5.16198×10^{-10}	1.08951×10^{-10}	2.21184×10^{-11}
0.09	3.25780×10^{-9}	7.52497×10^{-10}	2.50264×10^{-9}	3.54294×10^{-11}
0.10	4.37568×10^{-9}	1.05421×10^{-9}	2.43280×10^{-10}	5.40000×10^{-11}

Table 5. The $|\ \Omega^5(\alpha,\tau)-\Omega^4(\alpha,\tau)\ |$ of Problem 2 at varying values of $\hbar$ at $\alpha=1.0$ determined by the ARPSM at plausible locations in the range $\tau\in[0,\ 0.10]$.

τ	$\hbar=0.7$	$\hbar=0.8$	$\hbar=0.9$	$\hbar=1.0$
0.01	6.68516×10^{-15}	3.24000×10^{-16}	1.48559×10^{-17}	6.48000×10^{-19}
0.02	7.56340×10^{-14}	5.18400×10^{-15}	3.36151×10^{-16}	2.07360×10^{-17}
0.03	3.12634×10^{-13}	2.62440×10^{-14}	2.08423×10^{-15}	1.57464×10^{-16}
0.04	8.55701×10^{-13}	8.29440×10^{-14}	7.60623×10^{-15}	6.63552×10^{-16}
0.05	1.86856×10^{-12}	2.02500×10^{-13}	2.07618×10^{-14}	2.02500×10^{-15}
0.06	3.53705×10^{-12}	4.19904×10^{-13}	4.71607×10^{-14}	5.03885×10^{-15}
0.07	6.06674×10^{-12}	7.77924×10^{-13}	9.43715×10^{-14}	1.08909×10^{-14}
0.08	9.68115×10^{-12}	1.32710×10^{-12}	1.72109×10^{-13}	2.12337×10^{-14}
0.09	1.46205×10^{-11}	2.12576×10^{-12}	2.92409×10^{-13}	3.82638×10^{-14}
0.10	2.11403×10^{-11}	3.24000×10^{-12}	4.69785×10^{-13}	6.48000×10^{-14}

Table 6. The $|\ \Omega^6(\alpha,\tau)-\Omega^5(\alpha,\tau)\ |$ of Problem 4.2 at varying values of $\hbar$ at $\alpha=1.0$ determined by the ARPSM at plausible locations in the range $\tau\in[0,\ 0.10]$.

τ	$\hbar=0.7$	$\hbar=0.8$	$\hbar=0.9$	$\hbar=1.0$
0.01	5.70140×10^{-18}	1.36875×10^{-19}	3.07037×10^{-21}	6.48000×10^{-23}
0.02	1.04787×10^{-16}	3.81301×10^{-18}	1.29644×10^{-19}	4.14720×10^{-21}
0.03	5.75296×10^{-16}	2.66996×10^{-17}	1.15783×10^{-18}	4.72392×10^{-20}
0.04	1.92590×10^{-15}	1.06221×10^{-16}	5.47412×10^{-18}	2.65421×10^{-19}
0.05	4.91650×10^{-15}	3.10013×10^{-16}	1.82654×10^{-17}	1.01250×10^{-18}
0.06	1.05735×10^{-14}	7.43789×10^{-16}	4.88885×10^{-17}	3.02331×10^{-18}
0.07	2.02020×10^{-14}	1.55881×10^{-15}	1.12388×10^{-16}	7.62366×10^{-18}
0.08	3.53965×10^{-14}	2.95907×10^{-15}	2.31140×10^{-16}	1.69869×10^{-17}
0.09	5.80497×10^{-14}	5.20820×10^{-15}	4.36616×10^{-16}	3.44374×10^{-17}
0.10	9.03612×10^{-14}	8.63622×10^{-15}	7.71241×10^{-16}	6.48000×10^{-17}

Table 7. The $|\ \Omega^4(\alpha,\tau)-\Omega^3(\alpha,\tau)\ |$ of Problem 4.3 at varying values of $\hbar$ at $\alpha=0.002$ when $\xi=2.0$ determined by the ARPSM at plausible locations in the range $\tau\in[0,\ 0.10]$.

τ	$\hbar=0.7$	$\hbar=0.8$	$\hbar=0.9$	$\hbar=1.0$
0.01	1.71234×10^{-5}	1.64238×10^{-6}	1.50887×10^{-7}	1.33333×10^{-8}
0.02	1.19254×10^{-4}	1.5092810^{-5}	1.82962×10^{-6}	2.13333×10^{-7}
0.03	3.71134×10^{-4}	5.52410×10^{-5}	7.87569×10^{-6}	1.08000×10^{-6}
0.04	8.30537×10^{-4}	1.38697×10^{-4}	2.21854×10^{-5}	3.41333×10^{-6}
0.05	1.55134×10^{-3}	2.83255×10^{-4}	4.95386×10^{-5}	8.33333×10^{-6}
0.06	2.58472×10^{-3}	5.07642×10^{-4}	9.54985×10^{-5}	1.72800×10^{-5}

Table 7. *Cont.*

τ	$\hbar = 0.7$	$\hbar = 0.8$	$\hbar = 0.9$	$\hbar = 1.0$
0.07	3.97984×10^{-3}	8.31357×10^{-4}	1.66343×10^{-4}	3.20133×10^{-5}
0.08	5.78419×10^{-3}	1.27456×10^{-3}	2.69015×10^{-4}	5.46133×10^{-5}
0.09	8.04396×10^{-3}	1.85802×10^{-3}	4.11079×10^{-4}	8.74800×10^{-5}
0.10	1.08042×10^{-2}	2.60300×10^{-3}	6.00692×10^{-4}	1.33333×10^{-4}

Table 8. The $\mid \Omega^5(\alpha, \tau) - \Omega^4(\alpha, \tau) \mid$ of Problem 4.3 at varying values of $\hbar$ at $\alpha = 0.002$ when $\xi = 2.0$ determined by the ARPSM at plausible locations in the range $\tau \in [0,\ 0.10]$.

τ	$\hbar = 0.7$	$\hbar = 0.8$	$\hbar = 0.9$	$\hbar = 1.0$
0.01	2.75110×10^{-7}	1.33333×10^{-8}	6.11355×10^{-10}	2.66667×10^{-11}
0.02	3.11251×10^{-6}	2.13333×10^{-7}	1.38334×10^{-8}	8.53333×10^{-10}
0.03	1.28656×10^{-5}	1.08000×10^{-6}	8.57707×10^{-8}	6.48000×10^{-9}
0.04	3.52140×10^{-5}	3.41333×10^{-6}	3.13014×10^{-7}	2.73067×10^{-8}
0.05	7.68955×10^{-5}	8.33333×10^{-6}	8.54394×10^{-7}	8.33333×10^{-8}
0.06	1.45558×10^{-4}	1.72800×10^{-5}	1.94077×10^{-6}	2.07360×10^{-7}
0.07	2.49660×10^{-4}	3.20133×10^{-5}	3.88360×10^{-6}	4.48187×10^{-7}
0.08	3.98401×10^{-4}	5.46133×10^{-5}	7.08269×10^{-6}	8.73813×10^{-7}
0.09	6.01665×10^{-4}	8.74800×10^{-5}	1.20333×10^{-5}	1.57464×10^{-6}
0.10	8.69973×10^{-4}	1.33333×10^{-4}	1.93327×10^{-5}	2.66667×10^{-6}

Table 9. The $\mid \Omega^6(\alpha, \tau) - \Omega^5(\alpha, \tau) \mid$ of Problem 4.3 at varying values of $\hbar$ at $\alpha = 1.0$ when $\xi = 2.0$ determined by the ARPSM at plausible locations in the range $\tau \in [0,\ 0.10]$.

τ	$\hbar = 0.7$	$\hbar = 0.8$	$\hbar = 0.9$	$\hbar = 1.0$
0.01	7.82086×10^{-9}	1.87757×10^{-10}	4.21175×10^{-12}	8.88889×10^{-14}
0.02	1.43741×10^{-7}	5.23046×10^{-9}	1.77838×10^{-10}	5.68889×10^{-12}
0.03	7.89157×10^{-7}	3.66250×10^{-8}	1.58824×10^{-9}	6.48000×10^{-11}
0.04	2.64184×10^{-6}	1.45708×10^{-7}	7.50908×10^{-9}	3.64089×10^{-10}
0.05	6.74417×10^{-6}	4.25257×10^{-7}	2.50554×10^{-8}	1.38889×10^{-9}
0.06	1.45041×10^{-5}	1.02029×10^{-6}	6.70624×10^{-8}	4.14720×10^{-9}
0.07	2.77119×10^{-5}	2.13829×10^{-6}	1.54167×10^{-7}	1.04577×10^{-8}
0.08	4.85548×10^{-5}	4.05908×10^{-6}	3.17065×10^{-7}	2.33017×10^{-8}
0.09	7.96293×10^{-5}	7.14430×10^{-6}	5.98925×10^{-7}	4.72392×10^{-8}
0.10	1.23952×10^{-4}	1.18467×10^{-5}	1.05794×10^{-6}	8.88889×10^{-8}

Table 10. The Abs. E of Problem 1 at $\alpha = 0.003$ when $\hbar = 1.0$ in the range $\tau \in [0,\ 0.10]$.

τ	$\lvert\Omega(\alpha, \tau) - \Omega^5(\alpha, \tau)\rvert$	$\lvert\Omega(\alpha, \tau) - \Omega^6(\alpha, \tau)\rvert$	$\lvert\Omega(\alpha, \tau) - \Omega^7(\alpha, \tau)\rvert$
0.01	8.30269×10^{-19}	2.60496×10^{-20}	2.11758×10^{-22}
0.02	5.26512×10^{-17}	3.30768×10^{-18}	5.38461×10^{-20}
0.03	5.94281×10^{-16}	5.60646×10^{-17}	1.37022×10^{-18}
0.04	3.30894×10^{-15}	4.16685×10^{-16}	1.35902×10^{-17}
0.05	1.25095×10^{-14}	1.97128×10^{-15}	8.0436×10^{-17}
0.06	3.70206×10^{-14}	7.00821×10^{-15}	3.43448×10^{-16}
0.07	9.25270×10^{-14}	2.04572×10^{-14}	1.17061×10^{-15}
0.08	2.04357×10^{-13}	5.16919×10^{-14}	3.38332×10^{-15}
0.09	4.10678×10^{-13}	1.16989×10^{-13}	8.62135×10^{-15}
0.10	7.66068×10^{-13}	2.42728×10^{-13}	1.98913×10^{-14}

Table 11. The Abs. E of Problem 2 at $\alpha = 1.0$ when $\hbar = 1.0$ in the range $\tau \in [0,\ 0.10]$.

τ	$\lvert\Omega(\alpha,\tau) - \Omega^5(\alpha,\tau)\rvert$	$\lvert\Omega(\alpha,\tau) - \Omega^6(\alpha,\tau)\rvert$	$\lvert\Omega(\alpha,\tau) - \Omega^7(\alpha,\tau)\rvert$
0.01	2.94909×10^{-17}	2.94903×10^{-18}	2.95987×10^{-19}
0.02	4.40186×10^{-16}	4.42354×10^{-17}	4.80186×10^{-18}
0.03	7.67615×10^{-15}	7.69784×10^{-16}	7.60615×10^{-17}
0.04	7.11237×10^{-14}	7.19910×10^{-15}	7.10037×10^{-16}
0.05	5.63785×10^{-13}	5.46438×10^{-14}	5.12785×10^{-15}
0.06	1.03216×10^{-12}	1.00614×10^{-13}	1.00216×10^{-14}
0.07	6.41848×10^{-11}	5.72459×10^{-12}	6.11848×10^{-13}
0.08	1.47451×10^{-10}	3.12250×10^{-11}	3.01250×10^{-12}
0.09	1.07553×10^{-9}	7.28584×10^{-10}	1.01553×10^{-11}
0.10	1.23165×10^{-8}	5.89806×10^{-9}	1.03165×10^{-10}

Table 12. The Abs. E of Problem 3 at $\alpha = 1.0$ when $\hbar = 1.0$ in the range $\tau \in [0,\ 0.10]$.

τ	$\lvert\Omega(\alpha,\tau) - \Omega^5(\alpha,\tau)\rvert$	$\lvert\Omega(\alpha,\tau) - \Omega^6(\alpha,\tau)\rvert$	$\lvert\Omega(\alpha,\tau) - \Omega^7(\alpha,\tau)\rvert$
0.01	8.88178×10^{-14}	2.22045×10^{-16}	0.0
0.02	5.65636×10^{-12}	3.24185×10^{-14}	0.0
0.03	6.42488×10^{-11}	5.51115×10^{-13}	4.21885×10^{-15}
0.04	3.59969×10^{-10}	4.11982×10^{-12}	4.10783×10^{-14}
0.05	1.36929×10^{-9}	1.95961×10^{-11}	2.45359×10^{-13}
0.06	4.07716×10^{-9}	7.00426×10^{-11}	1.05249×10^{-12}
0.07	1.02521×10^{-8}	2.05550×10^{-10}	3.60423×10^{-12}
0.08	2.27795×10^{-8}	5.22144×10^{-10}	1.04659×10^{-11}
0.09	4.60513×10^{-8}	1.18793×10^{-9}	2.67941×10^{-11}
0.10	8.64113×10^{-8}	2.47757×10^{-9}	6.21085×10^{-11}

6. Conclusions

Graphs and numerical statistics were used to show the effectiveness of the ARPSM. As can be seen from the graphs and tables, the approximate solutions obtained using the ARPSM are in perfect agreement with the corresponding exact solutions. Tables 1–9 provide the numerical support for the convergence of the approximative exact solutions. Tables 10–12 present the comparative study in terms of the Abs. E of the approximate and exact solutions obtained using the proposed approach.

The important features of the ARPSM, as demonstrated by solving BSDEs, are as follows: The main benefit of the suggested approach is how quickly the coefficients of terms in a series solution may be calculated using the limit at infinity concept. Other well-known approximate analytical techniques, such as the RPSM, require that unknown coefficients in series solutions be determined using the fractional derivative and the VIM, ADM, and HPM, which call for the integration operators, which is difficult in the fractional case. He's or Adomian polynomials do not need the ARPSM to solve the problems. As a result, the ARPSM is a good replacement tool for He's or Adomian-polynomial-based methods because it requires incredibly few calculations to solve FODEs. As a result of the findings, we came to the conclusion that our approach is accurate and simple to use. To achieve the solution in the original space, the ARPSM must first determine the AT of the target equations and then execute the inverse AT. Therefore, the source functions for nonhomogeneous equations must be piecewise continuous and of exponential order, and after the calculations, the inverse AT must exist. Furthermore, it is assumed in this approach that the Caputo derivative satisfies the semi-group property.

It is significant to consider that implementing the ARPSM to solve other kinds of ordinary and partial FODEs of non-integer order is actively attainable. Our goal in the future is to apply the ARPSM to other systems of FODEs that arise in other areas of science.

Author Contributions: M.I.L., A.A. and H.A.-Z. declare that the study was realized in collaboration with equal responsibility. All authors have read and agreed to the published version of the manuscript.

Funding: This research received no external funding.

Data Availability Statement: No data were generated nor analyzed during the current study.

Acknowledgments: The authors thank the Editor and Reviewers for their suggestions.

Conflicts of Interest: The authors declare no conflict of interest.

References

1. Pandey, S.C. The Lorenzo-Hartley[s] function for fractional calculus and its applications pertaining to fractional order modelling of anomalous relaxation in dielectrics. *Comput. Appl. Math.* **2018**, *37*, 2648–2666. [CrossRef]
2. Tarasov, V.E. On history of mathematical economics: Application of fractional calculus. *Mathematics* **2019**, *7*, 509. [CrossRef]
3. Wang, Q.; Shi, X.; He, J.H.; Li, Z.B. Fractal calculus and its application to explanation of biomechanism of polar bear hairs. *Fractals* **2018**, *26*, 1850086. [CrossRef]
4. Nisar, K.S.; Suthar, D.L.; Agarwal, R.; Purohit, S.D. Fractional calculus operators with Appell function kernels applied to Srivastava polynomials and extended Mittag-Leffler function. *Adv. Differ. Equ.* **2020**, *2020*, 1–14. [CrossRef]
5. He, J.H. Fractal calculus and its geometrical explanation. *Results Phys.* **2018**, *10*, 272–276. [CrossRef]
6. Alidousti, J.; Ghahfarokhi, M.M. Stability and bifurcation for time delay fractional predator prey system by incorporating the dispersal of prey. *Appl. Math. Model.* **2019**, *72*, 385–402. [CrossRef]
7. Xu, C.; Liao, M.; Li, P.; Guo, Y.; Liu, Z. Bifurcation properties for fractional order delayed BAM neural networks. *Cogn. Comput.* **2021**, *13*, 322–356. [CrossRef]
8. Rihan, F.A.; Rajivganthi, C. Dynamics of fractional-order delay differential model of prey-predator system with Holling-type III and infection among predators. *Chaos Solitons Fractals* **2020**, *141*, 110365. [CrossRef]
9. Rezapour, S.; Liaqat, M.I.; Etemad, S. An Effective New Iterative Method to Solve Conformable Cauchy Reaction-Diffusion Equation via the Shehu Transform. *J. Math.* **2022**, *2022*, 4172218. [CrossRef]
10. Bas, E.; Ozarslan, R. Real world applications of fractional models by Atangana–Baleanu fractional derivative. *Chaos Solitons Fractals* **2018**, *116*, 121–125. [CrossRef]
11. Li, M.; Wang, J. Representation of solution of a Riemann–Liouville fractional differential equation with pure delay. *Appl. Math. Lett.* **2018**, *85*, 118–124. [CrossRef]
12. Traore, A.; Sene, N. Model of economic growth in the context of fractional derivative. *Alex. Eng. J.* **2020**, *59*, 4843–4850. [CrossRef]
13. Liaqat, M.I.; Khan, A.; Akgl, A.; Ali, M. A Novel Numerical Technique for Fractional Ordinary Differential Equations with Proportional Delay. *J. Funct. Spaces* **2022**, *2022*, 6333084. [CrossRef]
14. Jmal, A.; Elloumi, M.; Naifar, O.; Ben Makhlouf, A.; Hammami, M.A. State estimation for nonlinear conformable fractional-order systems: A healthy operating case and a faulty operating case. *Asian J. Control.* **2020**, *22*, 1870–1879. [CrossRef]
15. Hu, X.; Yuan, H.; Zou, C.; Li, Z.; Zhang, L. Co-estimation of state of charge and state of health for lithium-ion batteries based on fractional-order calculus. *IEEE Trans. Veh. Technol.* **2018**, *67*, 10319–10329. [CrossRef]
16. Wang, S.; He, S.; Yousefpour, A.; Jahanshahi, H.; Repnik, R.; Perc, M. Chaos and complexity in a fractional-order financial system with time delays. *Chaos Solitons Fractals* **2020**, *131*, 109521. [CrossRef]
17. Macas-Daz, J.E. Fractional CalculusTheory and Applications. *Axioms* **2022**, *11*, 43. [CrossRef]
18. Aba, Oud, M.A.; Ali, A.; Alrabaiah, H.; Ullah, S.; Khan, M.A.; Islam, S. A fractional order mathematical model for COVID-19 dynamics with quarantine, isolation, and environmental viral load. *Adv. Differ. Equ.* **2021**, *2021*, 1–19.
19. Esmaeili, S.; Shamsi, M. A pseudo-spectral scheme for the approximate solution of a family of fractional differential equations. *Commun. Nonlinear Sci. Numer. Simul.* **2011**, *16*, 3646–3654. [CrossRef]
20. Hasan, S.; El-Ajou, A.; Hadid, S.; Al-Smadi, M.; Momani, S. Atangana–Baleanu fractional framework of reproducing kernel technique in solving fractional population dynamics system. *Chaos Solitons Fractals* **2020**, *133*, 109624. [CrossRef]
21. Akinfe, T.K.; Loyinmi, A.C. A solitary wave solution to the generalized Burgers-Fisher's equation using an improved differential transform method: A hybrid scheme approach. *Heliyon* **2021**, *7*, e07001. [CrossRef] [PubMed]
22. Maleknejad, K.; Basirat, B.; Hashemizadeh, E. A Bernstein operational matrix approach for solving a system of high order linear VolterraFredholm integro-differential equations. *Math. Comput. Model.* **2012**, *55*, 1363–1372. [CrossRef]
23. Odibat, Z.; Momani, S. The variational iteration method: An efficient scheme for handling fractional partial differential equations in fluid mechanics. *Comput. Math. Appl.* **2009**, *58*, 2199–2208. [CrossRef]
24. Abdeljawad, T.; Amin, R.; Shah, K.; Al-Mdallal, Q.; Jarad, F. Efficient sustainable algorithm for numerical solutions of systems of fractional order differential equations by Haar wavelet collocation method. *Alex. Eng. J.* **2020**, *59*, 2391–2400. [CrossRef]
25. Wang, B.S.; Li, P.; Gao, Z.; Don, W.S. An improved fifth order alternative WENO-Z finite difference scheme for hyperbolic conservation laws. *J. Comput. Phys.* **2018**, *374*, 469–477. [CrossRef]
26. Liaqat, M.I.; Khan, A.; Akgl, A. Adaptation on power series method with conformable operator for solving fractional order systems of nonlinear partial differential equations. *Chaos Solitons Fractals* **2022**, *157*, 111984. [CrossRef]
27. Xiang, W.; Yan, S.; Wu, J.; Niu, W. Dynamic response and sensitivity analysis for mechanical systems with clearance joints and parameter uncertainties using Chebyshev polynomials method. *Mech. Syst. Signal Process.* **2020**, *138*, 106596. [CrossRef]
28. Bayrak, M.A.; Demir, A. A new approach for space-time fractional partial differential equations by residual power series method. *Appl. Math. Comput.* **2018**, *336*, 215–230.

29. Ahmad, I.; Zaman, S. Local meshless differential quadrature collocation method for time-fractional PDEs. D*Iscrete Contin. Dyn. Syst. S* **2020**, *13*, 2641. [CrossRef]
30. Kabir, H.; Aghdam, M.M. A generalized 2D Bzier-based solution for stress analysis of notched epoxy resin plates reinforced with graphene nanoplatelets. *Thin-Walled Struct.* **2021**, *169*, 108484. [CrossRef]
31. Liaqat, M.I.; Akgl, A. A novel approach for solving linear and nonlinear time-fractional Schrdinger equations. *Chaos Solitons Fractals* **2022**, *162*, 112487. [CrossRef]
32. Nuugulu, S.M.; Gideon, F.; Patidar, K.C. A robust numerical solution to a time-fractional Black–Scholes equation. *Adv. Differ. Equ.* **2021**, *2021*, 1–25. [CrossRef]
33. De Staelen, R.H.; Hendy, A.S. Numerically pricing double barrier options in a time-fractional Black–Scholes model. *Comput. Math. Appl.* **2017**, *74*, 1166–1175. [CrossRef]
34. Dubey, V.P.; Kumar, R.; Kumar, D. A reliable treatment of residual power series method for time-fractional Black–Scholes European option pricing equations. *Phys. A Stat. Mech. Its Appl.* **2019**, *533*, 122040. [CrossRef]
35. Yavuz, M.; zdemir, N. A different approach to the European option pricing model with new fractional operator. *Math. Model. Nat. Phenom.* **2018**, *13*, 12. [CrossRef]
36. Kadalbajoo, M.K.; Tripathi, L.P.; Kumar, A. A cubic B-spline collocation method for a numerical solution of the generalized Black–Scholes equation. *Math. Comput. Model.* **2012**, *55*, 1483–1505. [CrossRef]
37. Ankudinova, J.; Ehrhardt, M. On the numerical solution of nonlinear Black–Scholes equations. *Comput. Math. Appl.* **2008**, *56*, 799–812. [CrossRef]
38. Golbabai, A.; Nikan, O.; Nikazad, T. Numerical analysis of time fractional Black–Scholes European option pricing model arising in financial market. *Comput. Appl. Math.* **2019**, *38*, 1–24. [CrossRef]
39. Sarboland, M.; Aminataei, A. On the numerical solution of time fractional Black–Scholes equation. *Int. J. Comput. Math.* **2022**, *99*, 1736–1753. [CrossRef]
40. Edeki, S.O.; Jena, R.M.; Chakraverty, S.; Baleanu, D. Coupled transform method for time-space fractional Black–Scholes option pricing model. *Alex. Eng. J.* **2020**, *59*, 3239–3246. [CrossRef]
41. Ghandehari, M.A.M.; Ranjbar, M. European option pricing of fractional version of the Black–Scholes model: Approach via expansion in series. *Int. J. Nonlinear Sci.* **2014**, *17*, 105–110.
42. Kanth, A.R.; Aruna, K. Solution of time fractional Black–Scholes European option pricing equation arising in financial market. *Nonlinear Eng.* **2016**, *5*, 269–276.
43. Edeki, S.O.; Ugbebor, O.O.; Owoloko, E.A. Analytical solution of the time-fractional order Black–Scholes model for stock option valuation on no dividend yield basis. *IAENG Int. J. Appl. Math.* **2017**, *47*, 1–10.
44. Alfaqeih, S.; Ozis, T. Solving fractional Black–Scholes Eruopean option pricing equations by Aboodh transform Decomposition method. *Palest. J. Math.* **2020**, *9*, 915–924.
45. Kumar, S.; Kumar, D.; Singh, J. Numerical computation of fractional Black–Scholes equation arising in financial market. *Egypt. J. Basic Appl. Sci.* **2014**, *1*, 177–183. [CrossRef]
46. Liaqat, M.I.; Etemad, S.; Rezapour, S.; Park, C. A novel analytical Aboodh residual power series method for solving linear and nonlinear time-fractional partial differential equations with variable coefficients. *AIMS Math.* **2022**, *7*, 16917–16948. [CrossRef]
47. Aboodh, K.S. The New Integral Transform'Aboodh Transform. *Glob. J. Pure Appl. Math.* **2013**, *9*, 35–43.
48. Liaqat, M.I.; Khan, A.; Alam, M.; Pandit, M.K. A Highly Accurate Technique to Obtain Exact Solutions to Time-Fractional Quantum Mechanics Problems with Zero and Nonzero Trapping Potential. *J. Math.* **2022**, *2022*, 9999070. [CrossRef]
49. Jena, R.M.; Chakraverty, S. Q-homotopy analysis Aboodh transform method based solution of proportional delay time-fractional partial differential equations. *J. Interdiscip. Math.* **2019**, *22*, 931–950. [CrossRef]
50. Alquran, M. Analytical solutions of fractional foam drainage equation by residual power series method. *Math. Sci.* **2014**, *8*, 153–160. [CrossRef]
51. Az-Zo'bi, E.A.; Yildirim, A.; Al Zoubi, W.A. The residual power series method for the one-dimensional unsteady flow of a van der Waals gas. *Phys. A Stat. Mech. Its Appl.* **2019**, *517*, 188–196. [CrossRef]
52. Wang, L.; Chen, X. Approximate analytical solutions of time fractional Whitham-Broer-Kaup equations by a residual power series method. *Entropy* **2015**, *17*, 6519–6533. [CrossRef]

Disclaimer/Publisher's Note: The statements, opinions and data contained in all publications are solely those of the individual author(s) and contributor(s) and not of MDPI and/or the editor(s). MDPI and/or the editor(s) disclaim responsibility for any injury to people or property resulting from any ideas, methods, instructions or products referred to in the content.